ARTICLE NO. 79-1516R

J80-096

0009
0016
0001

Subsonic Flow Past an Oscillating Cascade with Finite Mean Flow Deflection

Joseph M. Verdon* and Joseph R. Caspar*
United Technologies Research Center, East Hartford, Conn.

A theoretical model for predicting the aerodynamic response due to a finite-deflection cascade oscillating in a subsonic stream is described. Based on the assumption of small amplitude harmonic blade motions, the unsteady flow is treated as a small fluctuation about the nonuniform mean flow. The mean or steady flow is determined as a solution of the full potential equation while the unsteady flow is governed by a linear equation with variable coefficients which depend on the steady flow field. Numerical solutions based on this general aerodynamic model have been obtained for simple cascade configurations. Selected results for sharp-edged blade profiles are described. Those for flat plate cascades are shown to be in good agreement with previous analytical predictions for both subresonant and superresonant blade motions. Predictions for double circular arc and thin circular arc profiles reveal that blade thickness has a significant effect on the unsteady response while the effect of flow turning due to blade camber is only minimal.

Introduction

SUPERSONIC unstalled flutter and subsonic positive incidence flutter (often called subsonic stalled flutter) are the two most commonly observed aeroelastic instabilities occurring in modern fans and compressors.[1] Extensive analytical and experimental work has been reported on the problem of supersonic unstalled flutter, and solutions of the classical small disturbance equations (e.g., Refs. 2, 3) have been shown to be remarkably successful at predicting the observed flutter behavior of supersonic test fans.[1,4] As a result, it is generally believed that the development of a supersonic unstalled flutter prediction system is well in hand. In contrast, for subsonic flow, the classical approach has not provided practically useful flutter predictions and it appears that a more comprehensive aerodynamic model will be required. In particular, recent experimental evidence[1] indicates that flow separation or stalling is not an essential condition for the appearance of positive incidence flutter; hence, an unsteady formulation which includes the effects of mean flow deflection due to blade thickness and steady loading could be sufficient for predicting the onset of subsonic flutter in fans and compressors. Such a model would also be applicable to the flutter analysis of thick, highly cambered turbine blades. Minimum requirements for a useful model are the capability of treating high Mach number subsonic flow and of providing efficient numerical predictions of unsteady response coefficients.

Although substantial progress has been achieved in the development of unsteady subsonic cascade solutions, to date these have been largely based on classical linear theory and are thus confined to flat plate blades at zero mean incidence relative to a uniform stream (e.g., Refs. 5-7). Such solutions do not reveal instabilities under practical operating conditions, and hence fail to meet the needs of turbomachinery designers for predicting or understanding the occurrence of subsonic flutter. Nishiyama and Kobayashi[8] and Namba[9] have extended the classical model in an attempt to include the effect of relative displacement of blades with finite mean circulation. Both analyses employ identical linearizations to arrive at linear constant coefficient steady and unsteady boundary value problems and determine analytical solutions for flat plate blades at small but finite incidence relative to the inlet flow direction. However, the conditions under which this linearization is valid are at best restrictive,[9] thus limiting the practical utility of these solutions.

In contrast to the foregoing analytical studies, a compressible unsteady aerodynamic model which fully includes the effects of nonuniform mean flow will require numerical solution procedures. One effort in this direction is that due to Ni and Sisto.[10] They regarded the fluid properties as dependent variables and applied an explicit time-marching procedure to determine solutions to the Euler equations of motion. However, the computing time required by this time-marching formulation renders it unacceptable for detailed and repetitive flutter calculations. Verdon et al.[11] have provided a preliminary unsteady subsonic cascade formulation in which the velocity potential is treated as the basic dependent variable. The steady flow is determined as a solution of the full nonlinear potential equation and the unsteady flow is governed by linear, time-independent equations with variable coefficients. Similar linearizations with respect to a nonuniform steady flow have been applied by Guiraud-Vallee et al.[12] to obtain numerical solutions for subsonic and transonic flow past oscillating airfoils in channels, and by Atassi and Akai[13] to derive analytic solutions for incompressible flow past a cascade of Joukowski airfoils.

The present paper describes a continuation of the work reported in Ref. 11. Basic equations which govern the flow in a single extended blade-passage region of a finite-deflection two-dimensional oscillating cascade are outlined. The derivation essentially involves a perturbation expansion of the velocity potential leading to a nonlinear boundary value problem for the zeroth order or steady flow potential and a linear variable coefficient boundary value problem for the first order or unsteady potential. The coefficients in the unsteady problem depend on the underlying steady flow. Numerical solutions for the steady problem are available for subsonic[14] and transonic[15] flows, while solution procedures for the unsteady problem are under current development. To

Received June 1, 1979; presented as Paper 79-1516 at the AIAA 12th Fluid and Plasma Dynamics Conference, Williamsburg, Va., July 23-25, 1979; revision received Sept. 5, 1979.

Index categories: Nonsteady Aerodynamics; Subsonic Flow; Airbreathing Propulsion.

*Senior Research Engineer, Computational Fluid Dynamics. Member AIAA.

date, unsteady solutions have been obtained for flat plate cascades and cascades of sharp-edged circular arc blades. A selection of these results are described in this paper. Although progress towards the development of an aerodynamic analysis for investigating subsonic flutter in turbomachines is being achieved, a number of difficult problems remain to be resolved and substantial further work will be required before a useful flutter prediction system can be realized.

Description of the Problem

In the following discussion all quantities are dimensionless. Lengths have been scaled with respect to blade chord, time with respect to the ratio of blade chord to upstream free stream speed, and pressure with respect to the upstream free stream dynamic pressure. Consider isentropic and irrotational flow, with negligible body forces, of a perfect gas past a two-dimensional oscillating cascade (Fig. 1). These restrictions lead to a single nonlinear differential equation for the velocity potential $\hat{\Phi}(X,t)$ and an explicit algebraic equation for the fluid pressure $\hat{P}(X,t)$; i.e.,

$$\hat{A}^2 \nabla^2 \hat{\Phi} = \hat{\Phi}_{tt} + 2\nabla\hat{\Phi}\cdot\nabla\hat{\Phi}_t + \nabla\hat{\Phi}\cdot\nabla(\nabla\hat{\Phi})^2/2 \tag{1}$$

$$\hat{P} = P_{-\infty} - 2[1-(M_{-\infty}\hat{A})^{2\gamma/(\gamma-1)}]/(\gamma M^2_{-\infty}) \tag{2}$$

where X is a position vector extending from the origin of the space-fixed x,y-coordinate system (Fig. 1), $M_{-\infty}<1$ and $P_{-\infty}$ are the upstream free stream Mach number and pressure, respectively, γ is the specific heat ratio of the fluid, and the speed of sound propagation $\hat{A}$ is given by

$$(M_{-\infty}\hat{A})^2 = 1-(\gamma-1)M^2_{-\infty}\{\hat{\Phi}_t + [(\nabla\hat{\Phi})^2 - 1]/2\} \tag{3}$$

Only subsonic solutions are sought here, but the basic equations described below also apply to transonic flows with weak shocks.

The blades of the cascade have finite thickness, camber, and mean incidence angle relative to the inlet flow, and are undergoing identical small-amplitude harmonic motions at frequency ω and constant interblade phase angle σ. The mean or steady state positions of the blade chord lines coincide with the line segments $mG_x \le x \le 1+mG_x$, $y=mG_y$, $m=0, \pm 1, \pm 2,\ldots$, where G_x- and G_y are the x and y components of the cascade gap vector $\boldsymbol{G}$, which is directed along the locus of blade leading edges with magnitude equal to the blade spacing (Fig. 1). Blade shape and orientation relative to the stream, and the amplitude and frequency of the blade motion, are assumed to be such that the flow remains attached to the blade surface; i.e.,

$$(\nabla\hat{\Phi}\cdot\boldsymbol{n})_{\mathcal{S}_m} = \partial\mathfrak{R}_m/\partial t\cdot\boldsymbol{n}_{\mathcal{S}_m}, \quad m=0,\pm1,\pm2,\ldots \tag{4}$$

Here $\mathfrak{R}_m$ is a vector measuring the displacement of points on the instantaneous position of the mth blade surface $\mathcal{S}_m$ relative to their mean positions, and $\boldsymbol{n}$ is a unit outward normal vector. In addition to Eq. (4), the fluid pressure and normal velocity must be continuous across wake surfaces $\mathcal{W}_m$. In the inviscid approximation the wakes are represented by thin vortex sheets, each of which emanates from a point in the vicinity of a blade trailing edge and extends downstream. In the far field the flow consists of unsteady fluctuations, due to outward acoustic wave propagation and vorticity convection (downstream), about uniform inlet and exit conditions.

For rigid blade motions the relative displacement vector is given by

$$\mathfrak{R}_m = re^{i(\omega t+m\sigma)} = (\boldsymbol{h}+\boldsymbol{\alpha}\times\boldsymbol{R}_p)e^{i(\omega t+m\sigma)}, \quad m=0,\pm1,\pm2,\ldots \tag{5}$$

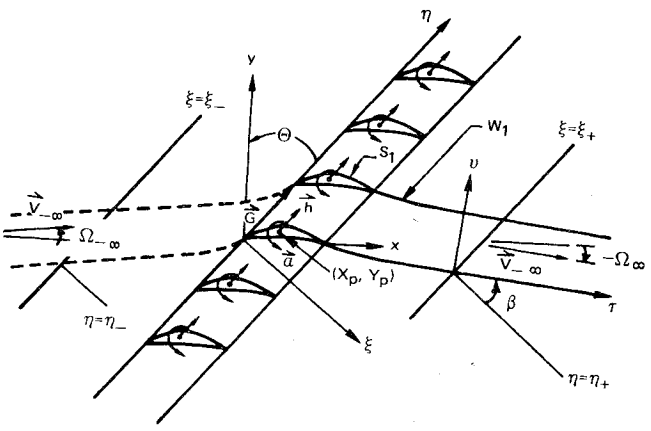

Fig. 1 Two-dimensional oscillating cascade with finite mean flow deflection-extended blade passage region and far-field parameters.

where $\boldsymbol{h}$ defines the amplitude and direction of blade translations, α defines the amplitude of blade rotations about axes with mean positions located at (X_p+mG_x, Y_p+mG_y), and $\boldsymbol{R}_p$ is a vector extending from the mean position of the mth axis of rotation to points on the mean position of the mth blade surface S_m. Only rigid motions are considered; however, the present formulation could be readily extended to include elastic deformations of the blades. The components h_x, h_y, and α of the vectors $\boldsymbol{h}$ and $\boldsymbol{\alpha}$ are, in general, complex to permit phase differences between the translations in the x- and y-directions and the rotation. These rigid two-dimensional motions describe chordwise, bending, and torsional vibrations of actual rotor blades.

Perturbation Procedure

The velocity potential is expanded in an asymptotic series in ϵ:

$$\hat{\Phi}(X,t) = \sum_{j=0}^{\infty}\epsilon^j\phi_j(X,t) = \Phi(X) + \epsilon\phi(X)e^{i\omega t} + \mathcal{O}(\epsilon^2) \tag{6}$$

where ϵ is a small parameter related to the amplitude of the blade motion by

$$\epsilon = \max_{S_m}|\mathfrak{R}_m| = \max_{S}(\boldsymbol{r}\cdot\boldsymbol{r}^*)^{1/2} \tag{7}$$

In Eq. (7), * denotes the complex conjugate and S denotes the zeroth or reference blade surface. After substituting the foregoing series into the differential equation governing the fluid motion [Eq. (1)], equating terms with like powers in ϵ and, finally, neglecting terms of second and higher order in ϵ, a nonlinear equation for the zeroth order potential and a linear, variable coefficient equation for the first order potential are obtained. A similar procedure is applied to the expressions for the blade and wake boundary conditions. In addition, Taylor series expansions, e.g.,

$$\hat{\Phi}_{\mathcal{S}_m} = \hat{\Phi}_{S_m} + (\mathfrak{R}_m\cdot\nabla)\hat{\Phi}|_{S_m} + \mathcal{O}(\epsilon^2) \tag{8}$$

are applied to refer boundary conditions to the mean positions of the blade and wake surfaces. The mean positions W_m of the unsteady wakes are assumed to coincide with the steady flow stagnation streamlines.

As $\epsilon\to0$ the blade and wake surface collapse to their mean positions. Hence, the zeroth order term in the power series expansion [Eq. (6)] is the velocity potential $\Phi(X)$ due to steady flow past a stationary cascade. The cascade geometry, the prescribed form of the blade motion, and the linearity of the first order equations require that the first order or unsteady potential be harmonic in time [i.e., $\phi_1(X,t)=\phi(X)e^{i\omega t}$] and that the steady and first order un-

steady flows exhibit blade-to-blade periodicity:

$$\left.\begin{aligned}\Phi(X) &= \Phi(X+mG) - V_{-\infty}\cdot G \\ \phi(X) &= \phi(X+mG)e^{-im\sigma}\end{aligned}\right\} \quad m=0,\pm 1,\pm 2,\ldots \qquad (9)$$

The periodicity conditions permit boundary value problems for the steady and unsteady flows to be specified for a single extended blade-passage region of the cascade.

Restrictions implied by the perturbation approximation are usually not satisfied in the vicinity of blade edges. Such local violations of the assumptions indicate that the perturbation expansion is singular; i.e., the asymptotic series [Eq. (6)] is not uniformly valid throughout the flow.[16] In classical theory, in which the linearization is based on a uniform mean flow, a manifestation of this situation is the square root singularity in the unsteady pressure at blade leading edges. Singular behavior associated with the coupling of the steady and unsteady flows is not clearly understood at present and remains as a subject for future investigation.

Steady and Unsteady Boundary Value Problems

The perturbation approach serves to replace the nonlinear, time-dependent boundary value problem for the full potential $\hat{\Phi}(X,t)$ by two time-independent boundary value problems for the zeroth order or steady potential $\Phi(X)$ and the first order or unsteady potential $\phi(X)e^{i\omega t}$. Equations governing the steady potential follow from the differential equation [Eq. (1)] the speed-of-sound relation [Eq. (3)], and the flow tangency condition [Eq. (4)], after replacing $\hat{\Phi}(X,t)$ by $\Phi(X)$ and omitting time derivative terms. The steady flow tangency condition is applied at the upper, S_0^+, and lower, S_1^-, surfaces of the zeroth and first blade, respectively. The steady solution on the reference passage periodic boundaries upstream and downstream of the blade row is determined by the zeroth order differential equation and the blade-to-blade periodicity condition. Finally, since steady subsonic velocities are very nearly equal to the free stream velocity beyond some finite distance upstream or downstream of the blade row (e.g., $\xi<\xi_-$ or $\xi>\xi_+$ in Fig. 1), a uniform velocity approximation, i.e.,

$$\nabla\Phi = V_{\mp\infty}, \quad \xi \lessgtr \xi_{\mp} \qquad (10)$$

is used to provide far-field conditions for the steady boundary value problem.

The Linear Unsteady Model

It follows from Eqs. (1), (3), and (6) that the unsteady potential is governed by a linear differential equation of the form

$$\mathcal{L}\{\phi\} = \sum_{j,k=0}^{j+k\le 2} C_{jk}(X)\frac{\partial^{j+k}\phi}{\partial x^j \partial y^k} = 0 \qquad (11)$$

where

$$\begin{aligned} C_{00} &= \omega^2 - i\omega(\gamma-1)\nabla^2\Phi \\ C_{10} &= -[2i\omega + (\gamma-1)\nabla^2\Phi]\Phi_x - 2\nabla\Phi\cdot\nabla\Phi_x \\ C_{01} &= -[2i\omega + (\gamma-1)\nabla^2\Phi]\Phi_y - 2\nabla\Phi\cdot\nabla\Phi_y \\ C_{20} &= A^2 - \Phi_x^2, \quad C_{11} = -2\Phi_x\Phi_y, \quad C_{02} = A^2 - \Phi_y^2 \end{aligned} \qquad (12)$$

and A is the speed of sound in the steady flow. The influence of blade shape and incidence relative to the free stream appears in this equation through the variable coefficients $C_{jk}(X)$, which depend on the spatial derivatives of the steady potential. Upon substituting the series expansions [Eq. (6) and (8)] into the flow tangency relation, [Eq. (4)] and noting that $n_S = n_S + (\alpha\times n_S)e^{i\omega t} + \mathcal{O}(\epsilon^2)$, it follows after some algebra that the first order flow tangency condition has the form

$$\epsilon\nabla\phi\cdot n = [i\omega r + \alpha\times\nabla\Phi - (r\cdot\nabla)\nabla\Phi]\cdot n e^{im\sigma}, \quad \text{on } S_m, m=0,\pm 1,\pm 2,\ldots \qquad (13)$$

Finally, the conditions of continuity of pressure and normal velocity across blade wakes and the blade-to-blade periodicity of the unsteady flow require that

$$\left.\begin{aligned} i\omega\Delta_m\phi + \nabla\Phi\cdot\nabla(\Delta_m\phi) &= 0 \\ \nabla(\Delta_m\phi)\cdot n &= 0\end{aligned}\right\} \text{ on } W_m, m=0,\pm 1,\pm 2,\ldots \qquad (14)$$

where $\Delta_m\phi$ is the difference in potential across the mth wake, i.e.,

$$\Delta_m\phi \equiv \phi(X^-) - \phi(X^+) = \phi(X^- + G)e^{-i\sigma} - \phi(X^+), \quad X \text{ on } W_m \qquad (15)$$

The unsteady potential in the extended reference passage [i.e., the region bounded by the upper and lower surfaces of the zeroth and first blade, respectively, and by the zeroth and first steady flow stagnation streamlines (Fig. 1)] is determined as a solution of the variable coefficient differential equation [Eq. (11)], subject to the flow tangency requirement [Eq. (13)] at the upper S_0^+ and lower S_1^- surfaces of the zeroth and first blades, and the continuity conditions [Eq. (14)] across the zeroth wake W_0. The unsteady velocity is continuous and differentiable upstream of the blade row and, hence, the blade-to-blade periodicity condition [Eq. (9)] is used in conjunction with the unsteady differential equation to determine the values of the unsteady potential on the upstream stagnation streamlines. To complete the specification of the unsteady boundary value problem, conditions at upstream and downsteam boundaries of the extended blade passage region must be established.

Unsteady Far-Field Solutions

In general, unsteady disturbances do not attenuate in the far field of the cascade, and hence it is difficult to place explicit conditions on the unsteady potential ϕ at upstream and downstream boundaries of the extended blade passage region. Instead, analytic far-field solutions based on the uniform steady velocity approximation [Eq. (10)] have been determined for subsonic inlet and exit conditions. When the steady velocity field is uniform the coefficients of the steady differential equation [Eq. (11)] assume constant values. Solutions of this constant coefficient equation subject to appropriate boundary conditions can be matched to the near-field numerical solutions at finite distances upstream and downstream of the blade row (e.g., on the lines $\xi=\xi_{\mp}$ in Fig. 1). The analytic far-field solutions thus serve to complete the specification of the unsteady boundary value problem.

The unsteady potential is continuous upstream and has both continuous and discontinuous components downstream of the blade row. The continuous potential must satisfy the requirements of blade-to-blade periodicity and outgoing acoustic wave propagation at infinity. Fourier methods can be used to provide expressions for the continuous component of the far-field potential in terms of the independent variables ξ and η where ξ,η-coordinate axes are perpendicular and parallel, respectively, to the cascade inlet plane, and the origin of this coordinate system coincides with that of the x,y-system (Fig. 1). For subsonic inlet and exit conditions the continuous potential can be written as[11]

$$\phi_c(\xi,\eta) = \sum_{j=-\infty}^{\infty} b_j \exp(iq_j\eta) \times \exp[(iM_{-\infty}V_\xi\delta_j \pm d_j)(\xi-\xi_{\mp})/Q^2], \quad \xi \lessgtr \xi_{\mp} \qquad (16)$$

where

$$q_j=(2\pi j+\sigma)/G, \quad \delta_j=M_{-\infty}(\omega+V_\eta q_j),$$

$$Q^2=M^2_{-\infty}(A^2-V^2_\xi)>0 \quad d_j^2=(Q^2q_j^2-\delta_j^2)M^2_{-\infty}A^2 \quad (17)$$

V_ξ and V_η are the components of the uniform steady velocity in the ξ- and η-coordinate directions, and $G=|G|$ is the cascade gap distance. The Fourier coefficients b_j are obtained from the relation

$$b_j=G^{-1}\int_\eta^{\eta+G}\phi_c(\xi,\eta)\exp(-iq_j\eta)\,d\eta, \quad \xi=\xi_\mp \quad (18)$$

The discontinuous component of the unsteady potential far downstream results from the counter vorticity shed from the trailing edges of the blades and convected along the blade wakes. After assuming that far downstream of the blade row the steady velocity field is uniform and hence the steady flow stagnation streamlines (the mean positions of the unsteady wakes) can be approximated by an array of parallel straight lines, the following closed form solution for the discontinuous potential can be determined:[11]

$$\phi_d(\tau,\upsilon)=-\Delta\phi(\xi_+,\eta_+)\exp(-i\omega\tau/V_\infty)$$

$$\times\left\{\frac{\exp(\omega\upsilon/V_\infty)}{1-\exp[(\omega/V_\infty-i\nu)G\cos\beta]}\right.$$

$$\left.+\frac{\exp(-\omega\upsilon/V_\infty)}{1-\exp[-(\omega/V_\infty+i\nu)G\cos\beta}\right\}, \quad 0<\upsilon<G\cos\beta \quad (19)$$

where τ and υ are Cartesian coordinates with the τ-axis coinciding with the far-downstream zeroth wake (Fig. 1), β denotes the angle through which the line $\eta=\eta_+$ must be rotated in the counterclockwise direction to coincide with the τ-axis, and ν is defined by

$$\nu=[\sigma+\omega\sin\beta/(GV_\infty)]/(G\cos\beta) \quad (20)$$

The expression for $\phi_c(\tau,\upsilon)$ given by Eqs. (19) and (20) provides the far-field wake vorticity distribution required to conserve circulation in the unsteady flow. It satisfies the unsteady differential equation in the far field (i.e, when $\phi=V_\infty\tau$) and the boundary conditions of blade-to-blade periodicity and continuous normal velocity and pressure across blade wakes.

The analytic far-field approximations to the unsteady potential permit a numerical analysis which treats a single extended blade-passage region of finite extent. This is an important factor in providing for an efficient numerical solution to the unsteady problem. The continous far-field solutions [Eqs. (16) and (17)] indicate that unsteady disturbances attenuate or persist in the far field depending on the sign of d_j^2. In classical theory there is no turning of the steady flow; $V_{-\infty}=V_\infty$, and the terms d_j^2, $j=0, \pm1, \pm2,...$ have the same values upstream and downstream of the blade row. Blade motions are called subresonant if disturbances attenuate in the far field ($d_j^2>0$ for all j) or superresonant if at least one acoustic mode persists far upstream and downstream of the cascade. Resonance is said to occur if $d_j=0$ for any j (Ref. 17) and one consequence of the classical theory is that a subsonic cascade cannot support an unsteady load when the blades are undergoing resonant oscillations.[8,18] The situation is somewhat obscured when the cascade turns the steady flow ($V_{-\infty}\neq V_\infty$) since disturbances may attenuate in one direction while propagating undiminished in the other. However, a natural extension of the previous classification is to label blade motions as subresonant if all disturbances damp out in the far field, and as superresonant if at least one disturbance mode persists either far upstream or downstream of the cascade. The consequences of an upstream or downstream resonance condition (i.e., $d_j=0$ for any j, $\xi\lesseqgtr\xi_\mp$) remain to be clarified.

Aerodynamic Response Coefficients

Solutions to the steady and unsteady boundary value problems are required to determine blade pressure distributions and aerodynamic force and moment coefficients. The pressure at the mth blade surface is given by [cf. Eq. (9)]

$$\hat{P}_{\mathcal{S}_m}=P_{\mathcal{S}}+\epsilon p_{\mathcal{S}}e^{i(\omega t+m\sigma)}+\mathcal{O}(\epsilon^2), \quad m=0,\pm1,\pm2,... \quad (21)$$

where P and $\epsilon pe^{i\omega t}$ are the zeroth (steady) and first (unsteady) order components of the fluid pressure, and $\mathcal{S}$ denotes the moving reference blade surface. After expanding the velocity potential $\hat{\Phi}(X,t)$ in the manner indicated by Eqs. (6) and (8) and substituting the result along with Eq. (21) into the pressure-potential relation [Eq. (2)], it follows that

$$P_{\mathcal{S}}=P_{-\infty}-2(\gamma M^2_{-\infty})^{-1}[1-(M_{-\infty}A)^{2\gamma/(\gamma-1)}]_S \quad (22)$$

and

$$p_{\mathcal{S}}=-2(M_{-\infty}A)^{2/(\gamma-1)}[i\omega\phi+\nabla\Phi\cdot\nabla\phi$$

$$+\epsilon^{-1}(r\cdot\nabla)(\nabla\Phi)^2/2]_S \quad (23)$$

Thus the steady and unsteady components of the pressure acting on a moving blade surface $\mathcal{S}_m$ are evaluated in terms of velocity potential information supplied at the mean position of the reference blade, S. The last term on the right-hand side of Eq. (23) measures the change in the steady pressure in the direction of the unsteady displacement, i.e.,

$$r\cdot\nabla P=-2(M_{-\infty}A)^{2/(\gamma-1)}r\cdot DV/Dt$$

$$=-2(M_{-\infty}A)^{2/(\gamma-1)}(r\cdot\nabla)(\nabla\Phi)^2/2 \quad (24)$$

The force and moment coefficients acting on the mth blade, i.e.,

$$\hat{C}_{F_m}=C_F+\epsilon c_F e^{i(\omega t+m\sigma)}+\mathcal{O}(\epsilon^2), \quad m=0,\pm1,\pm2,... \quad (25)$$

and

$$\hat{C}_{M_m}=C_M+\epsilon c_M e^{i(\omega t+m\sigma)}+\mathcal{O}(\epsilon^2), \quad m=0,\pm1,\pm2,... \quad (26)$$

are determined by simple integrations over the mean position of the reference blade. After some algebra it follows that the steady (C_F and C_M) and unsteady (c_F and c_M) force and moment coefficients are given by

$$C_F=-\oint_s P_{\mathcal{S}}n\,ds, \quad C_M=\oint_s P_{\mathcal{S}}R_p\cdot ds \quad (27)$$

and

$$c_F=-\oint_s P_{\mathcal{S}}n\,ds+\epsilon^{-1}\alpha\times C_F, \quad c_M=\oint_s P_{\mathcal{S}}R_p\cdot ds \quad (28)$$

where ds is a differential vector tangent to the mean blade surface. It should be noted that the moment is taken about the moving pitching axis. The unsteady force and moment coefficients are the important results of an aerodynamic analysis intended for flutter predictions. Knowledge of these coefficients permits the evaluation of aerodynamic work per cycle and/or aerodynamic damping, either of which can be used to determine whether the airstream supports or suppresses a prescribed blade motion.

Numerical Results

Solutions based on the foregoing aerodynamic model have been obtained for subsonic flow past oscillating cascades consisting of simple sharp-edged blade profiles. Steady flows have been calculated using the finite area numerical method developed by Caspar et al.[14] and solutions to the linear unsteady equations have been determined using a finite difference approximation. The calculation mesh employed for the unsteady case consists of contour curves which are averages of the bounding stagnation streamlines and lines which are parallel to the cascade inlet plane (Fig. 2). This mesh is body fitted and periodic, thereby facilitating the implementation of blade, wake, and cascade periodic boundary conditions, but it is nonorthogonal, thus disallowing the use of standard difference approximations. Instead, the unsteady potential is implicitly expanded in terms of polynomial functions (Fourier functions at far-field boundaries) at each mesh point by a least squares minimization of the error at neighboring mesh points. Differential equations and boundary conditions are approximated in this manner, resulting in a linear block tridiagonal system of algebraic equations which are solved directly using a block complex version of the Thomas algorithm.[19] Complete details of this unsteady numerical solution procedure will be provided in a future publication.

The unsteady results reported here were obtained using a mesh which consisted of 21 lines in the "streamwise" direction and 71 lines parallel to the cascade inlet plane. The distance along the chord between the 27 points distributed on the blade surface varied from 0.02 near blade leading and trailing edges to 0.05 at mid-chord. Analytic far-field solutions were matched to the numerical near-field solutions at a distance of two axial chords from the cascade inlet and exit planes, i.e., at $\xi = \xi_- = -2\cos\Theta$ and $\xi = \xi_+ = 3\cos\Theta$; far-field Fourier expansions [Eq. (16)] were truncated after $|j| = 8$. Approximately 75 seconds of CAU time on the UTRC UNIVAC 1110 Computer System were required for each unsteady solution; however, substantial reductions in computing time can be expected with further development of the computational procedure.

Unsteady pressure difference distributions and aerodynamic response coefficients will be presented for flat plate cascades and unstaggered cascades of symmetric double circular arc and thin circular arc blades undergoing single-degree-of-freedom plunging (bending) or pitching (torsional) oscillations. The unsteady pressure difference Δp is defined by

$$\Delta p(x,0) \equiv p_{s^-}(X) - p_{s^+}(X) = p_{s_I^-}(X+G)e^{-i\sigma} - p_{s^+}(X) \qquad 0 \le x \le l \tag{29}$$

When the imaginary parts of the plunging, h_y, and pitching, α, amplitudes are set equal to zero, the real and imaginary parts of the response coefficients Δp, c_L and c_M are in phase with the displacement and velocity of the blade surface, respectively. Thus, real parts of the coefficients represent values at the instants when the reference blade has reached its maximum positive displacement and its velocity is zero, and imaginary parts represent values at the instants when the reference blade is in its mean position and is moving at maximum velocity. The stability of single-degree-of-freedom bending motions with $\mathrm{Im}\{h_y\} = 0$ is governed by the sign of the imaginary part of the lift coefficient. If $\mathrm{Im}\{c_L\} < 0$, the airstream resists the blade motion, and hence this motion is stable according to linear theory. Similarly, if $\mathrm{Im}\{\alpha\} = 0$, single-degree-of-freedom torsional motions are stable when $\mathrm{Im}\{c_M\} < 0$.[20]

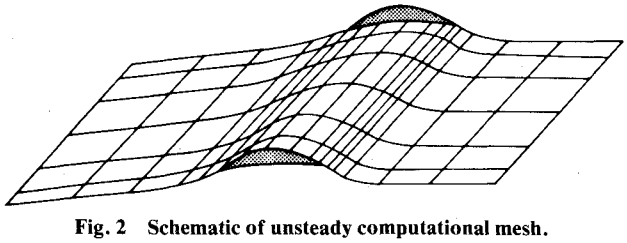

Fig. 2 Schematic of unsteady computational mesh.

Flat Plate Cascades

For oscillating flat plate cascades with blade mean positions aligned parallel to the freestream direction, $\Phi = x$, and the unsteady equations reduce to those of usual small disturbance theory. Response calculations have been performed to verify the present unsteady formulation, the analytic far field solutions in particular, and to assess the accuracy of the numerical solution procedure by comparing results against those of a well-established analytical solution.[7] Predictions have been obtained for a variety of cascade parameter combinations. Sample results for bending motions, $h_y = (1, 0)$, at $\omega = 1$, $M_{-\infty} = 0.7$, $G = 1$ and $\Theta = 45$ deg are shown in Figs. 3 and 4. Numerical and analytical predictions of pressure difference distributions (Fig. 3) for an out-of-phase ($\sigma = \pm\pi$) bending motion are in very good agreement except near the blade leading edge, where the finite difference approximation fails to capture the unsteady pressure singularity ($\Delta p \sim x^{-1/2}$). Rather than flow tangency conditions [Eq. (13)], wake boundary conditions [Eq. (14)] were applied in the numerical scheme at trailing edge points to achieve pressure closure; i.e., $\Delta p(1,0) = 0$ at the trailing edge. Agreement between numerical and analytical predictions has been observed to improve as free-stream Mach number is reduced. At low Mach number (e.g., $M = 0.3$) the numerical and analytical pressure difference predictions for out-of-phase bending motions, virtually coincide, except in the vicinity of the blade leading edge.

Lift coefficients due to bending are depicted in Fig. 4 for the entire range of interblade phase angles. For the example, cascade resonance occurs at $\sigma = -30$ deg and $\sigma = 107.8$ deg, and the blade motion is superresonant; in other words, unsteady disturbances persist in the far field for -30 deg $< \sigma <$ 107.8 deg. The lift coefficient distribution shown in Fig. 4 indicates that the present unsteady formulation ac-

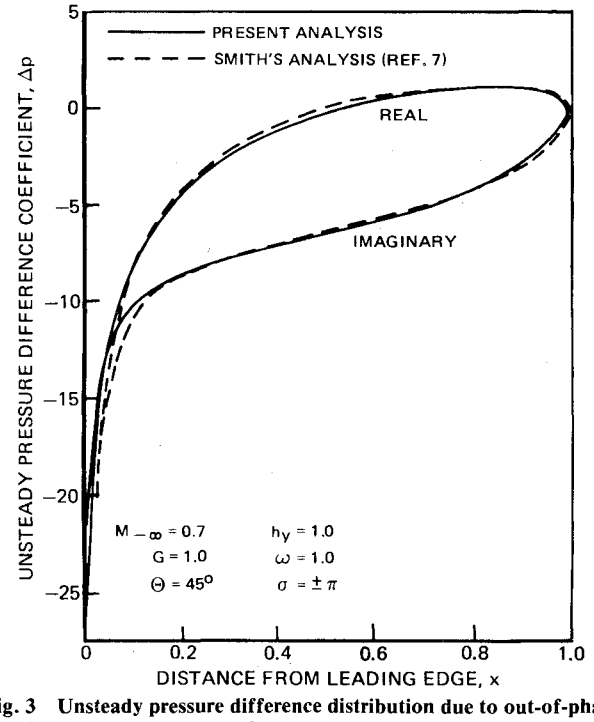

Fig. 3 Unsteady pressure difference distribution due to out-of-phase bending for a flat plate cascade.

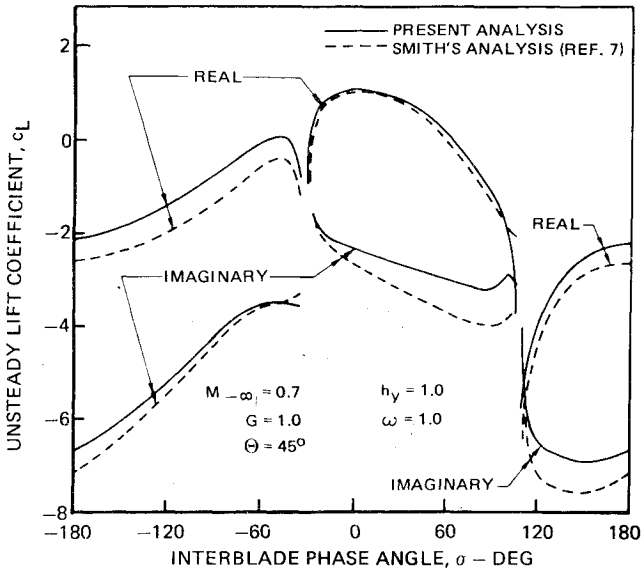

Fig. 4 Unsteady lift due to bending for a flat plate cascade.

curately models both subresonant and superresonant unsteady subsonic phenomena. In particular, the agreement between the present solution with the analytic solution of Smith indicates that the matching of the continuous component of the analytic far-field solution to the near field numerical solution provides an adequate representation of the effect of acoustic wave propagation into the far field. Again the differences between the numerical and analytical lift distributions (Fig. 4) are primarily attributed to the failure of the finite difference calculation to accurately predict singular behavior at blade leading edges. This has been clearly demonstrated by moment coefficient predictions in which the moments were taken about the leading edge to minimize the influence of the leading edge singularity. This singularity could be more accurately modeled by patching an analytical approximation to the unsteady potential in the vicinity of the leading edge into the numerical solution procedure.

Cascades of Circular Arc Blade Profiles

Oscillating cascades of sharp-edged symmetric double circular arc and thin circular arc blades have been considered in order to isolate and examine the effects of blade thickness and steady flow turning due to camber on the unsteady response. In general, blade stagger induces steady loading and therefore attention has been focused on unstaggered cascades. At present, incidence effects cannot be accurately evaluated because of the requirement of an extremely fine computational mesh in blade leading edge regions. Further, for sharp-edged blades incidence would cause leading edge separations in real flows and such phenomena have not been accounted for in the aerodynamic model.

The circular arc blade surfaces are defined by the equation

$$y = \pm F(x) = \pm\,[T/2 - R + \sqrt{R^2 - (x-0.5)^2}\,], \quad 0 \le x \le 1$$

$$R = (T^2+1)/4T \tag{30}$$

where R is the radius of curvature and $T/2$ is the half-thickness of the double circular arc profile, $y = \pm F(x)$, or the height of the thin circular arc profiles, $y = F(x)$. Predictions have been obtained for unstaggered cascades, $\Theta = 0$, with unit gap-chord ratio, $G = 1$, undergoing single-degree-of-freedom bending [$h_y = (1,0)$] or torsional [$\alpha = (1,0)$] vibrations at unit frequency, $\omega = 1$. The torsional axis is at mid-chord [$(X_p, Y_p) = (0.5,0)$] and in each case the free stream Mach number is 0.5. To avoid conditions which lead to infinite steady velocities at blade edges, inlet ($\Omega_{-\infty}$) and exit (Ω_{∞})

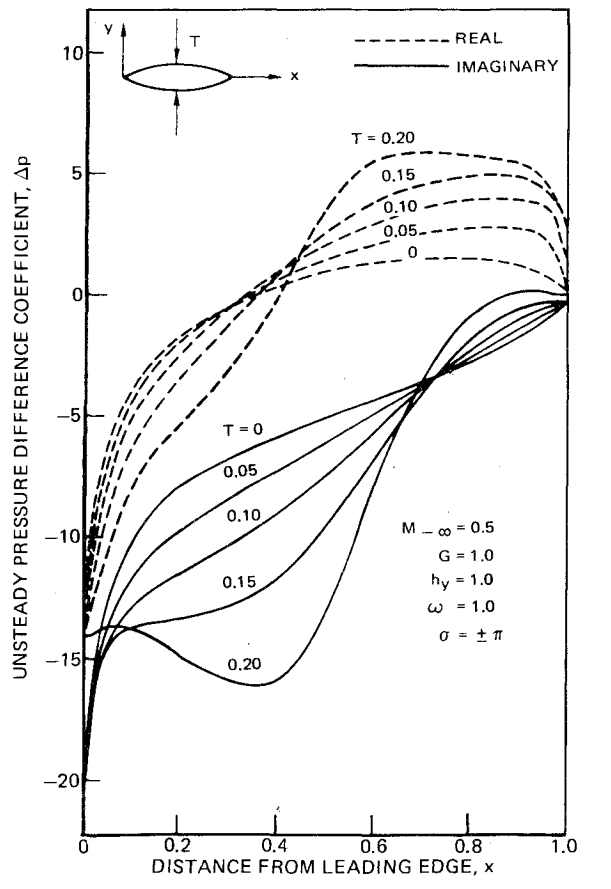

Fig. 5 Unsteady pressure difference distributions due to bending for unstaggered cascades of double circular arc airfoils.

flow angles (Fig. 1) have been determined by applying steady flow Kutta conditions at both leading and trailing edges: i.e,

$$V \cdot ds|_{s_m^-} = -V \cdot ds|_{s_m^+}, \quad x = 0,1 \tag{31}$$

where ds is the tangent to the blade surface and directed counterclockwise. For unstaggered double circular arc blades $\Omega_{-\infty} = \Omega_{\infty} = 0$ deg, but for thin circular arc blades the inlet and exit flow angles vary with the parameter T. For the cases considered here the inlet and exit flow angles are as follows: for $T = 0.05$, $\Omega_{-\infty} = -\Omega_{\infty} = 3.46$ deg; for $T = 0.1$, $\Omega_{-\infty} = -\Omega_{\infty} = 6.93$ deg; for $T = 0.15$, $\Omega_{-\infty} = -\Omega_{\infty} = 10.38$ deg; and for $T = 0.2$, $\Omega_{-\infty} = -\Omega_{\infty} = 13.8$ deg.

Unsteady pressure difference distributions for flat plate ($T = 0$), double circular arc, and thin circular arc blades are shown in Figs. 5-8. Pressure coefficient predictions for out-of-phase ($\sigma = \pm\pi$) bending and torsional vibrations of double circular arc blades (Figs. 5 and 6) reveal that blade thickness has a significant effect on unsteady response. However, the predictions for bending and torsional vibrations at $\sigma = -\pi/2$ of thin circular arc blades (Figs. 7 and 8) indicate that the effect of steady flow turning due to blade camber on the unsteady response is much less severe. For the double circular arc blades the variations of the real and imaginary pressure difference distributions due to bending and the real pressure difference distribution due to torsion are primarily due to the strong dependence on blade thickness of the steady, $\nabla\Phi$, and the unsteady, $\nabla\phi$, velocities at the blade surface [cf. Eq. (23)], particularly the latter. In addition, the relative displacement of the steady pressure field [the $(r \cdot \nabla)P$ term in Eq. (23)] also has an important influence on the real pressure difference distribution. Note that the numerical results do not indicate unsteady pressure closure [$\Delta p(1,0) = 0$] at the trailing edge. Although the accuracy of the numerical results is somewhat questionable in the vicinity of blade edges, in

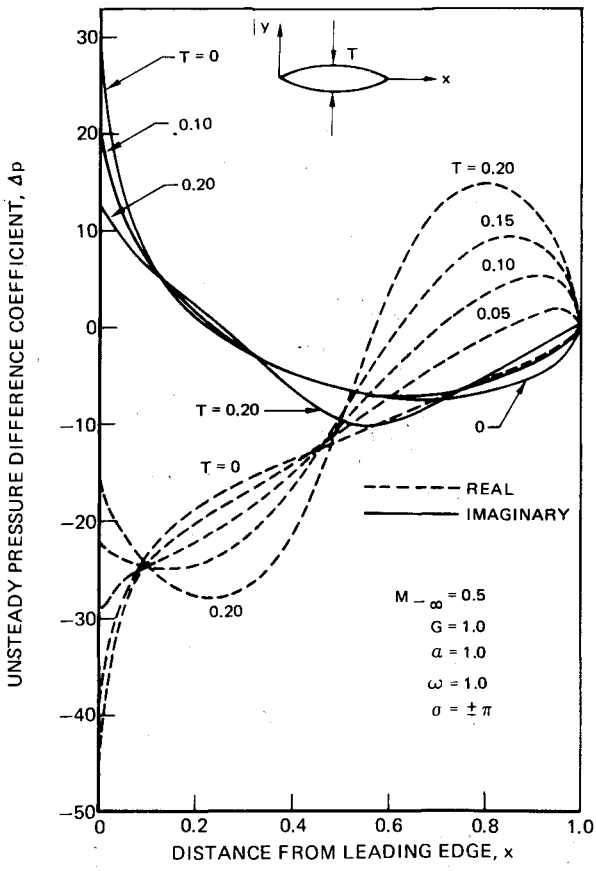

Fig. 6 Unsteady pressure difference distributions due to torsion about midchord for unstaggered cascades of double circular arc airfoils.

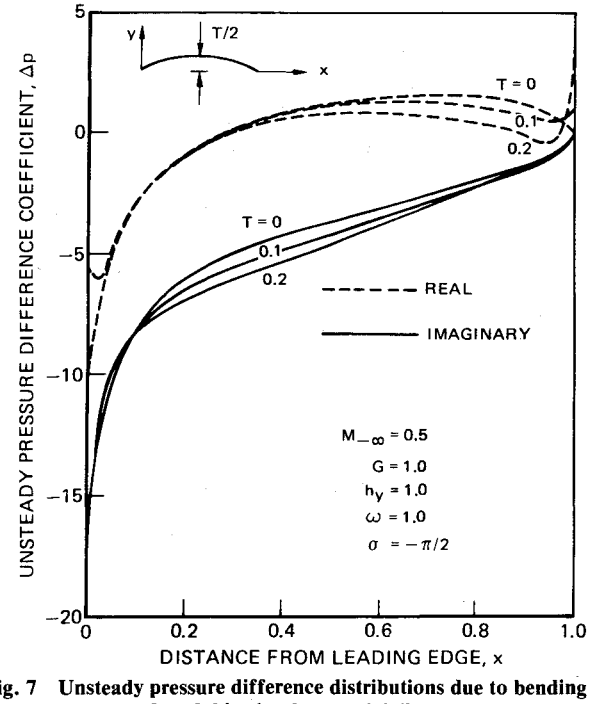

Fig. 7 Unsteady pressure difference distributions due to bending for unstaggered cascades of thin circular arc airfoils.

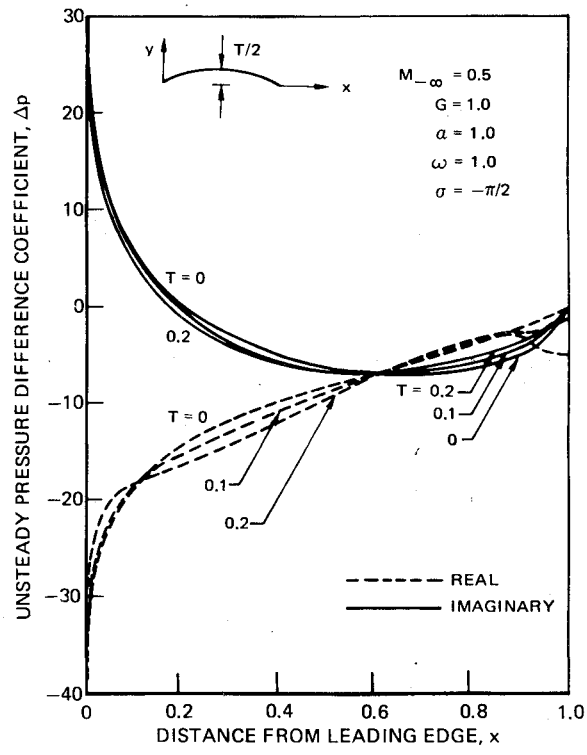

Fig. 8 Unsteady pressure difference distributions due to torsion about midchord for cascades of thin circular arc airfoils.

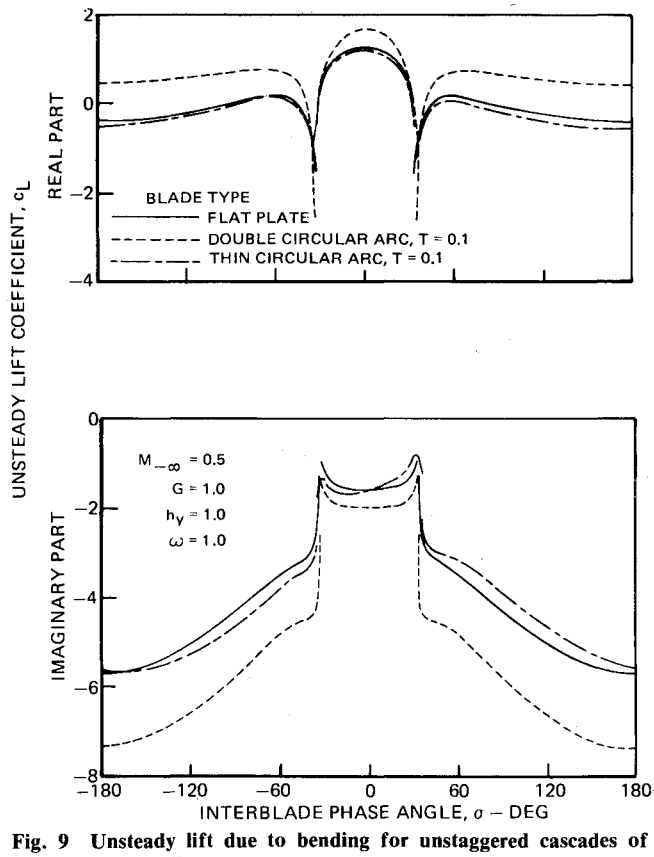

Fig. 9 Unsteady lift due to bending for unstaggered cascades of sharp-edged airfoils.

general, $\Delta p(1,0) \neq 0$, because upper and lower surface steady flow accelerations [cf. Eqs. (23) and (24)] are not equal at blade trailing edges.[21]

Unsteady lift and moment coefficients are plotted vs interblade phase angle for cascades of flat plate, 10%-thick double circular arc ($T=0.1$), and 5%-high thin circular arc ($T=0.1$) blades undergoing bending and torsional vibrations about midchord, respectively, in Figs. 9 and 10. For the flat plate and double circular arc blades the superresonant region of blade motions lies between $\sigma = \pm 33.1$ deg, while for the thin circular arc profiles this region lies between $\sigma = \pm 35.4$ deg. As indicated previously by the pressure difference

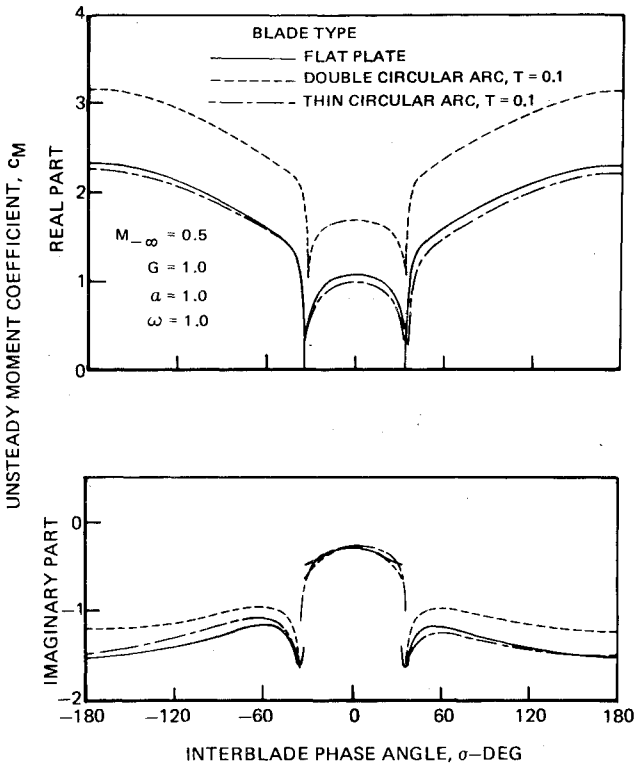

Fig. 10 Unsteady moment due to torsion about midchord for unstaggered cascades of sharp-edged airfoils.

predictions for out-of-phase motions (Figs. 5 and 6), blade thickness causes a significant change in the real and imaginary unsteady lift coefficients for bending vibrations (Fig. 9), and on the real part of the moment coefficient due to torsional motions (Fig. 10). In contrast, blade camber produces only small changes in unsteady lift and moment relative to flat plate results. The imaginary lift coefficient predictions for flat plate and circular arc airfoils depicted in Fig. 9 indicate that the effect of blade thickness is strongly stabilizing for single-degree-of-freedom bending vibrations (i.e., $\mathrm{Im}\{c_L\}$ decreases as blade thickness is increased), and that the effect of camber is slightly destabilizing for bending motions at positive interblade phase angles. The imaginary moment coefficient predictions (Fig. 10) indicate that the effect of thickness is destabilizing for subresonant torsional motions and that the effect of steady flow turning due to blade chamber is slightly destablizing for subresonant torsional motions at negative interblade phase angles. Single-degree-of-freedom bending or torsional vibrations at $\omega = 1$ are stable for the three example cascades. Superresonant motions are much closer to the stability boundary (i.e., $\mathrm{Im}\{c_L\}$ or $\mathrm{Im}\{c_M\} = 0$) than subresonant motions; however, the effects of both thickness and camber are less pronounced in the superresonant region.

Concluding Remarks

The aerodynamic model described in this paper fully accounts for the effects of blade geometry, namely thickness and camber, and of mean flow incidence on the unsteady response to an oscillating cascade in fully attached subsonic flow. This model has been derived by treating the unsteady flow as a small perturbation about nonuniform mean flow, and it can serve as a basis for investigating subsonic flutter phenomena in jet engine fan, compressor, and turbine blade rows. Numerical procedures for solving the subsonic unsteady boundary value problem have been developed to the extent that the effects of blade thickness and camber on unsteady response can now be examined. In this paper a limited number of results have been presented for cascades of sharp-edged blades undergoing single-degree-of-freedom bending or torsional vibrations. Accurate numerical predictions have been obtained for vibrating flat plate cascades over the entire range of interblade phase angles, i.e., for both subresonant and superresonant blade motions. Response predictions for symmetric double circular arc and thin circular arc profiles reveal that blade thickness produces a strong coupling between the steady and unsteady flows while steady blade loading (or flow turning) due solely to blade camber causes only weak steady-unsteady interactions.

Further developments in the aerodynamic model and the associated numerical solution procedures will be necessary before a comprehensive flutter prediction scheme can be realized. Numerical procedures must be improved so that general profile shapes (i.e., rounded or blunt-edged blades) and the effects of mean flow incidence can be considered. In addition, an effort should be initiated to better understand the implications of the leading and trailing edge singularities associated with the perturbation approach on unsteady force and moment predictions, and to assess the need for the development of a more rational, albeit more complicated, perturbation model for blade edge regions. Finally, for the subsonic Mach number range in which blade vibration problems are of practical concern, it will be necessary to extend the present analysis to include transonic flows with weak shocks, and for vibrating, thin fan or compressor blades at incidence (the positive incidence flutter problem) it appears that the aerodynamic model will have to be modified to incorporate leading edge, supersonic separation regions.

Acknowledgement

This research was sponsored in part by the Commerical Products Division, Pratt and Whitney Aircraft Group, United Technologies Corporation.

References

[1] Mikolajczak, A. A., Arnoldi, R. A., Snyder, L. E., and Stargardter, H., "Advances in Fan and Compressor Blade Flutter Analysis and Predictions," *Journal of Aircraft*, Vol. 12, April 1975, pp. 325-332.

[2] Verdon, J. M., "Flutter Developments in the Aerodynamic Analysis of Unsteady Supersonic Cascades: Parts 1 and 2," *Transactions of the ASME: Journal of Engineering for Power*, Ser. A., Vol. 99, Oct. 1977, pp. 509-525.

[3] Adamczyk, J. J., and Goldstein, M. E., "Unsteady Flow in a Supersonic Cascade with Subsonic Leading Edge Locus," *AIAA Journal*, Vol. 16, Dec. 1978, pp. 1248-1254.

[4] Snyder, L. E., and Commerford, G. L., "Supersonic Unstalled Flutter in Fan Rotors; Analytical and Experimental Results," *Transactions of the ASME: Journal of Engineering for Power*, Ser. A, Vol. 96, Oct. 1974, pp. 379-386.

[5] Whitehead, D. S., "Vibration and Sound Generation in a Cascade of Flat Plates in Subsonic Flow," R&M 3685, British Aeronautical Research Council, London, England, Feb. 1970.

[6] Kaji, S., and Okazaki, T., "Propagation of Sound Waves Through a Blade Row, II. Analysis Based on the Acceleration Potential Method," *Journal of Sound and Vibration*, Vol. 2, March 1970, pp. 335-375.

[7] Smith, S. N., "Discrete Frequency Sound Generation in Axial Flow Turbomachines," R&M 3709, British Aeronautical Research Council, London, England, 1971.

[8] Nishiyama, T., and Kobayashi, H., "Theoretical Analysis for Unsteady Characteristics of Oscillating Cascade Airfoils in Subsonic Flows," Technology Reports, Tohoku University, Vol. 38, July 1973, pp. 287-314.

[9] Namba, M., "Subsonic Cascade Flutter with Finite Mean Lift," *AIAA Journal*, Vol. 13, May 1975, pp. 586-593.

[10] Ni, R. H., and Sisto, F., "Numerical Computation of Nonstationary Aerodynamics of Flat Plate Cascades in Compressible Flow," *Transactions of the ASME: Journal of Engineering for Power*, Ser. A, Vol. 98, April 1976, pp. 165-170.

[11] Verdon, J. M., Adamczyk, J. J., and Caspar, J. R., "Subsonic Flow Past an Oscillating Cascade with Steady Blade Loading—Basic

Formulation," *Unsteady Aerodynamics*, edited by R. B. Kinney, proceedings of a symposium held at the University of Arizona, Tucson, Ariz., March 1975, Vol. 2, pp. 827-851.

[12] Guiraud-Vallee, D., et al., "Numerical Studies of Unsteady Inviscid Flows at ONERA," paper presented at the Conference on Numerical Methods and Fluid Dynamic Applications, University of Reading, England, Jan. 4-6, 1978.

[13] Atassi, H., and Akai, T. J., "Aerodynamic and Aeroelastic Characteristics of Oscillating Loaded Cascades at Low Mach Number, Part I. Pressure Distribution, Forces and Moments," ASME Paper 79-GT-111, 24th International Gas Turbine Conference, San Diego, Calif., March 12-15, 1979.

[14] Caspar, J. R., Hobbs, D. E., and Davis, R. L., "Calculation of Two-Dimensional Potential Cascade Flow Using Finite Area Methods," *AIAA Journal*, Vol. 18, Jan. 1980, pp. 103-109.

[15] Ives, D. C. and Liutermozza, J. F., "Analysis of Transonic Cascade Flow Using Conformal Mapping and Relaxation Techniques," *AIAA Journal*, Vol. 15, May 1977, pp. 647-652.

[16] Van Dyke, M., *Perturbation Methods in Fluid Mechanics*, Academic Press, New York, 1964, pp. 45-52.

[17] Samoilovich, G. S., "Resonance Phenomena in Sub- and Supersonic Flow Through an Aerodynamic Cascade," *Mekhanika Zhidkosti i Gaza*, Vol. 2, No. 3, 1967, pp. 143-144.

[18] Whitehead, D. S., "The Effect of Compressibility on Unstalled Torsional Flutter," R&M 3754, British Aeronautical Research Council, London, England, 1974.

[19] Van Dine, C. P., "An Algorithm for the Optimization of Trajectories with Associated Parameters," *AIAA Journal*, Vol. 7, March 1969, pp. 400-405.

[20] Fung, Y. C., *An Introduction to the Theory of Aeroelasticity*, Wiley, New York, 1955, pp. 166-168.

[21] Basu, B. C., and Hancock, G. J., "The Unsteady Motion of a Two-Dimensional Aerofoil in Incompressible Inviscid Flow," *Journal of Fluid Mechanics*, Vol. 87, Part 1, 1978, pp. 159-178.